



Mean potential energy change in stratified grid turbulence

Chris R. Rehmann^{a,*}, Jeffrey R. Koseff^b

^a *Department of Civil and Environmental Engineering, Hydrosystems Laboratory,
University of Illinois at Urbana-Champaign, Urbana, IL 61801, USA*

^b *Department of Civil and Environmental Engineering, Environmental Fluid Mechanics Laboratory,
Stanford University, Stanford, CA 94305, USA*

Accepted 23 September 2003

Abstract

Laboratory experiments are used to study the effect of stratification and molecular diffusivity on the mean potential energy change due to grid turbulence in a linearly stratified fluid. Two quantities that characterize the potential energy change are the mixing efficiency, defined as the ratio of the mean potential energy change and the work done by the grid on the fluid, and the eddy diffusivity. As the stratification strength, measured by a Richardson number, increases, the mixing efficiency increases in agreement with previous predictions, reaches a maximum of about 6%, and then remains constant for the range of Richardson number used. Results from the present experiments and previous experiments collapse onto a single curve of efficiency versus Richardson number if the methods of computing the efficiency are consistent. Also, the efficiencies in temperature-stratified water and salt-stratified water match within the experimental uncertainty. Like the mixing efficiency, eddy diffusivities do not depend on the molecular diffusivity. Eddy diffusivities decrease as the stratification becomes stronger, though the trend differs from that observed in other towed-grid experiments. One experiment with dynamically active, stable gradients of both temperature and salinity was performed to allow both components to experience the same stratification and stirring strength. Results from this experiment show evidence of differential mixing of temperature and salinity, but experiments with reduced heat losses are required to make definite conclusions.

© 2003 Elsevier B.V. All rights reserved.

Keywords: Turbulence; Stratification; Mixing efficiency; Eddy diffusivity; Molecular diffusivity

* Corresponding author. Tel.: +1-217-333-9077; fax: +1-217-333-0687.

E-mail address: rehmann@uiuc.edu (C.R. Rehmann).

1. Introduction

Evaluating the mean potential energy change caused by turbulence in a stratified fluid is important for several problems in oceanography. For example, oceanographers studying mixing in the ocean thermocline evaluate the mixing due to a turbulent patch (Gregg, 1987) or measure the mean vertical transport over long times (Ledwell et al., 1993). In these applications, the rate and efficiency of mixing depend on the relative stratification strength. Effects of molecular diffusion can also be important. When either temperature or salinity is unstably stratified, double diffusive phenomena can occur (e.g., Schmitt, 1994). Even when the temperature and salinity profiles are diffusively-stable, preferential transport of heat, or differential diffusion, can occur. Differential diffusion can complicate the interpretation of tracer studies (Gargett, 2003) and affect the mixing efficiency (Jackson and Rehmann, 2003a,b). To understand the effects of stratification and molecular diffusivity on overall mixing, we perform towed-grid experiments to examine the changes in the mean density profile due to grid turbulence.

The effect of stratification on grid turbulence has been studied extensively in water channels and wind tunnels (e.g. Lienhard and Van Atta, 1990; Yoon and Warhaft, 1990; Barrett and Van Atta, 1991; Liu, 1995), but the experiments that use steady flow past a fixed grid cannot be used to estimate the mean potential energy change (Gregg, 1987). However, experiments with a grid towed horizontally through a linearly-stratified fluid (Fig. 1; Britter, 1985; Rottman and Britter, 1986; Barrett and Van Atta, 1991) have been used to study the mixing efficiency, or flux Richardson number R_f , defined as the ratio of the mean potential energy change ΔPE during a turbulent event to the work W done to create the event:

$$R_f = \frac{\Delta PE}{W} \quad (1)$$

In these experiments, a linear density profile is established, and the initial value of the potential energy

$$PE = g \int_V z \rho \, dV, \quad (2)$$

is computed, where V is the volume of the fluid and z the vertical coordinate. While a grid of bars with mesh M is towed at speed U through the fluid to create turbulence, the work the grid does on the fluid is measured. After the turbulence decays, the final density profile is measured and R_f and eddy diffusivities can be computed.

Previous experiments and analyses apply to cases with weak to moderate stratification, measured by the grid Richardson number $Ri_0 = (N_0 M / U)^2$, where $N_0 = -(g / \rho_0) \partial \rho / \partial z)^{1/2}$ is the initial buoyancy frequency and ρ_0 is the mid-depth density. For weak stratification, a gradient-transport analogy (Britter, 1985) and an extension of Linden's (1979) entrainment arguments both yield

$$R_f \propto Ri_0 \quad (3)$$

For somewhat stronger stratification, Britter (1985) used results from the Lagrangian dispersion analysis of Pearson et al. (1983) and the plume dispersion measurements of Britter

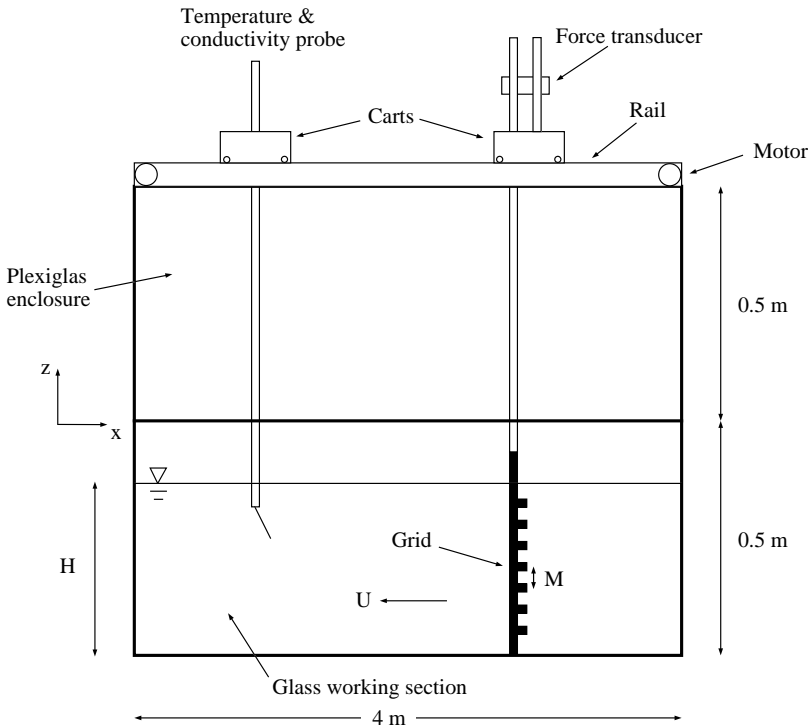


Fig. 1. Schematic diagram of the towed-grid experiment. In the present experiments, the water depth H was 35 cm, the tank width B was 80 cm, and the grid mesh M was 5.08 cm.

et al. (1983) to predict that

$$R_f \propto Ri_0^{1/2} \quad (4)$$

For $0.01 < Ri_0 < 0.8$ (Britter, 1985; Rottman and Britter, 1986), the data fit Britter's prediction (4) reasonably well. However, the exponent of a power law fit to data for $3 \times 10^{-3} < Ri_0 < 8 \times 10^{-3}$ (Barrett and Van Atta, 1991) falls between 0.5 and 1.0.

The behavior for even stronger stratification is less certain because mixing efficiencies for large Ri_0 are difficult to measure in a linearly-stratified fluid. For example, Rottman and Britter (1986) stated that their data tend to approach a constant but also said that they need more data to make a definite conclusion. Linden (1979) argued that since much of the work done on the fluid is used to generate internal waves when the stratification is strong, the efficiency should decrease. Thus, he proposed that the efficiency should rise from zero to a peak and decrease back to zero as the stratification becomes stronger. His compilation of measurements from several different flows supported this proposal, but only Linden's (1980) efficiency measurements with a grid dropped in a two-layer fluid displayed this behavior over the full range of stratification. Huq and Britter (1995) questioned some of Linden's (1980) assumptions about the volume over which the energy was input; their

results from experiments with a steady, two-layer flow past a vertical grid showed that the efficiency is nearly constant when the stratification is strong. Since they attributed the constant efficiency to sharpening of the interface between the layers, they suggested the efficiency should decrease for large Richardson number in a linearly-stratified fluid, which has no interface to sharpen. The form of the efficiency curve at high Richardson number is important because it can affect the formation of layers or finestructure in the ocean (Phillips, 1972; Posmentier, 1977). However, Balmforth et al. (1998) noted that layering depends on the method of supplying energy to the flow, and Holford and Linden (1999) argued that the Phillips–Posmentier mechanism does not cause the layering.

The magnitude of the mixing efficiency depends not only on the Richardson number but also on the process generating the turbulence. Linden's (1979) compilation shows that shear-induced mixing, such as that due to Kelvin–Helmholtz instability or in a mixing layer, has the highest efficiency. Both are examples of internal processes (Turner, 1979, Section 4.3), in which the energy for mixing is supplied where the mixing occurs. A grid, whether towed horizontally or dropped vertically (Linden, 1980), also supplies energy where the mixing occurs, but the energy is supplied independently of the flow. Thus, grid turbulence has a lower efficiency than other processes (Linden, 1979).

While effects of stratification have been studied for many years, effects of molecular diffusivity have recently received considerable attention because of the importance of differential diffusion for several oceanographic problems (Gargett, 2003). Laboratory, numerical, and oceanographic studies have provided evidence for differential transport of heat and salt, which in water have Schmidt numbers $Sc = \nu/D$ of 7 and 700, respectively, where ν is the kinematic viscosity and D is the molecular diffusivity of the scalar. Turner (1968) found that the entrainment of heat across a density interface exceeded the entrainment rate of salt when the stratification was strong. Since then several researchers have tried to determine the conditions under which molecular diffusion would affect the mixing (see Fernando, 1991). The numerical simulations of Merryfield et al. (1998) show greater transport of heat than salt for weak turbulence in a strongly stratified fluid. However, the experiments and simulations of Nagata and Komori (2001) show that the eddy diffusivity of a passive scalar—sodium fluorescein dye, which has $Sc = 600$ – 1200 (Nagata and Komori, 2001; Saylor and Sreenivasan, 1997)—exceeds that of active heat even for weak stratification. Field measurements by Nash and Moum (2002) show that the ratio K_S/K_T of the eddy diffusivities of salt and heat has a mean value of 0.7, but uncertainty in the measurements prevented a definitive conclusion about differential transport. Recently, Hebert and Ruddick (2003) measured differential diffusion of two dyes in a laboratory experiment on breaking internal waves, while Jackson and Rehmann (2003b) reported differential diffusion in a heat–salt system stirred with vertical rods.

We study the effects of stratification and molecular diffusivity on the overall mixing by examining the mixing efficiency and the eddy diffusivity of the turbulence. In particular, we measure the mixing efficiency over a wider range of Ri_0 than previously used and show that results from different experiments collapse to a single curve. To determine whether the molecular diffusivity affects overall mixing, we perform experiments with active gradients of heat, salt, or both. After describing the experimental procedures in Section 2, we present the measurements and compare with previous grid towing experiments in Section 3. We

discuss our laboratory results in terms of oceanographic applications in Section 4 and summarize the main conclusions in Section 5.

2. Experimental procedures and uncertainty

Experiments proceeded as follows: After a rectangular tank was filled and stratified with stable, linear distributions of salt, heat, or both, initial density profiles were measured with a conductivity–temperature probe. A grid was then towed through the water to create turbulence, and the work done by the grid was found by measuring the drag on the grid and integrating it over the length of the tow. After about five minutes, when the motions in the tank had decayed significantly, the grid was towed again. After a set of tows, the fluid was allowed to settle for about thirty minutes before profiles were measured at several locations in the direction of the towing along the centerline of the tank. Then, the potential energy change, mixing efficiency, and eddy diffusivity were computed. The conditions and results of the experiments are listed in Table 1.

The experimental facility (Fig. 1) consisted of a working section beneath a Plexiglas enclosure. The working section was 4 m long, 0.8 m wide, and 0.5 m deep. To reduce heat losses from the facility, the 6.4 mm glass inner walls were separated from the 6.4 mm Plexiglas outer walls by a 6.4 mm air gap. The bottom was similar, except that the in-

Table 1
Summary of conditions and results of the experiments

Experiment	Type	N (rad/s)	U (cm/s)	N_t	Re_M	Ri_0	R_f
1a	S	0.59	10.4	32	5300	8.36×10^{-2}	1.84×10^{-2}
2	S	0.92	5.1	72	2600	8.37×10^{-1}	4.64×10^{-2}
3	S	0.87	6.9	56	3500	4.09×10^{-1}	4.05×10^{-2}
4	S	0.37	20.0	16	10200	8.87×10^{-3}	5.78×10^{-3}
15	S	0.69	20.7	12	10500	2.86×10^{-2}	1.11×10^{-2}
16	S	0.79	9.1	30	4600	1.93×10^{-1}	3.28×10^{-2}
17	S	1.21	3.4	100	1700	3.26×10^0	5.54×10^{-2}
18	S	1.60	2.5	100	1300	1.07×10^1	5.01×10^{-2}
6a	H	0.31	4.9	12	2500	1.02×10^{-1}	3.04×10^{-2}
9	H	0.27	15.2	10	7700	8.10×10^{-3}	6.67×10^{-3}
10	H	0.26	18.9	8	9600	4.78×10^{-3}	5.13×10^{-3}
12	H	0.39	3.9	28	2000	2.60×10^{-1}	4.68×10^{-2}
13a	H	0.17	30.4	4	15400	8.49×10^{-4}	1.67×10^{-3}
5b	H	0.26	9.7	10	4900	1.80×10^{-2}	8.89×10^{-3}
6b	H	0.28	6.7	22	3400	4.33×10^{-2}	1.18×10^{-2}
13b	H	0.17	28.0	4	14200	9.03×10^{-4}	2.20×10^{-3}
8a	H	0.22	22.9	8	11600	2.47×10^{-3}	3.22×10^{-3}
19	SH	0.59	12.3	20	6300	5.91×10^{-2}	1.93×10^{-2}

The type of the experiment is salt ‘S’, heat ‘H’, or salt and heat ‘SH’. In experiment 19, the salinity gradient made up 59% of the initial density gradient, while the temperature gradient accounted for the other 41%. In all cases, the buoyancy frequency was computed from the linear portion of the initial density profile. The reference density ρ_0 was the average density of this portion, and the density gradient was taken as the slope of a least-squares line fit to the profile in this portion. The grid speed U is an average over all tows, N_t the total number of tows, and $Re_M = UM/\nu$ the grid Reynolds number.

ner wall was 12.7 mm thick glass. The bottom and sides were insulated with 7.5 cm of Styrofoam. The Plexiglas enclosure, which extended 0.5 m above the working section and supported the aluminum rails on which the grid and probe carts traveled, was insulated with plastic bubble wrap. The facility was filled to a depth of 35 cm and stratified using the double-bucket method. Food-grade sodium chloride was used in experiments with salinity stratification.

Density profiles were computed from temperature and conductivity profiles measured with a Precision Measurements Engineering model 125 conductivity–temperature probe, which consists of a Thermometrics FP07 thermistor mounted about 2 mm from a four-electrode conductivity sensor. The thermistor was calibrated with a Rosemount 162 platinum resistance thermometer, and the conductivity sensor was calibrated with solutions of known salinity. Profiles were measured from about 19 mm below the water surface to 9 mm above the tank bottom, filtered, and extrapolated to the boundaries using functions that satisfy no-flux conditions. The probe traveled at 10 cm s^{-1} , and its vertical position was taken as the product of the probe speed and the time elapsed since the probe started its travel. Density was computed from the salinity and temperature using the equation of state from [Ruddick and Shirtcliffe \(1979\)](#).

The grid had wooden, 1 cm square bars placed in a biplane configuration, a square mesh with a length of 5 cm, and a solidity of 36%. It was attached by a mast to a cart that traveled at speeds between 2.5 and 30 cm s^{-1} along rails on top of the Plexiglas enclosure. Above a hinge the mast bore against a Western Load Cell force transducer. The drag on the grid was computed by summing moments about the hinge, and the work done by the grid on the water was computed by integrating the drag over the length of the tow.

The grid was towed over 353 cm in sets of even numbers of tows to reduce any asymmetry in the mixing. To resolve the change in potential energy adequately, the number of tows in a set ranged from two for weak initial stratifications to twenty for stronger stratifications. Grid turbulence experiments (e.g., [Barrett and Van Atta, 1991](#)) show that turbulence decays in half a buoyancy period, or a maximum of 20 s in our experiments. Therefore, five minutes were allowed between tows in a set so that most of the turbulent and mean motion could decay before re-stirring the fluid. About thirty minutes were allowed between the last tow in a set and profiling so that internal waves could also decay. Tows continued usually until no part of the profile had the same gradient as the initial profile.

The mixing efficiency was computed from the measurements of the cumulative potential energy change and cumulative work done. The potential energy change after a total of n tows ΔPE was computed from (2) as

$$\Delta\text{PE} = gB \int_0^L \int_{-H}^0 z(\rho_n - \rho_{\text{in}}) dz dx, \quad (5)$$

where ρ_n is the density profile after n tows, ρ_{in} the initial density profile, and x is in the tow direction. This integral involved profiles measured at three to eight positions along the centerline of the facility. The efficiency can be taken as the slope of a line fit to ΔPE versus W , but because R_f would then be the average slope of the curve, it would depend on the level to which the fluid is mixed ([Fig. 2](#)). Including more points (i.e. more mixing) lowers the estimate of R_f . To compare efficiencies measured in runs mixed to different levels, we

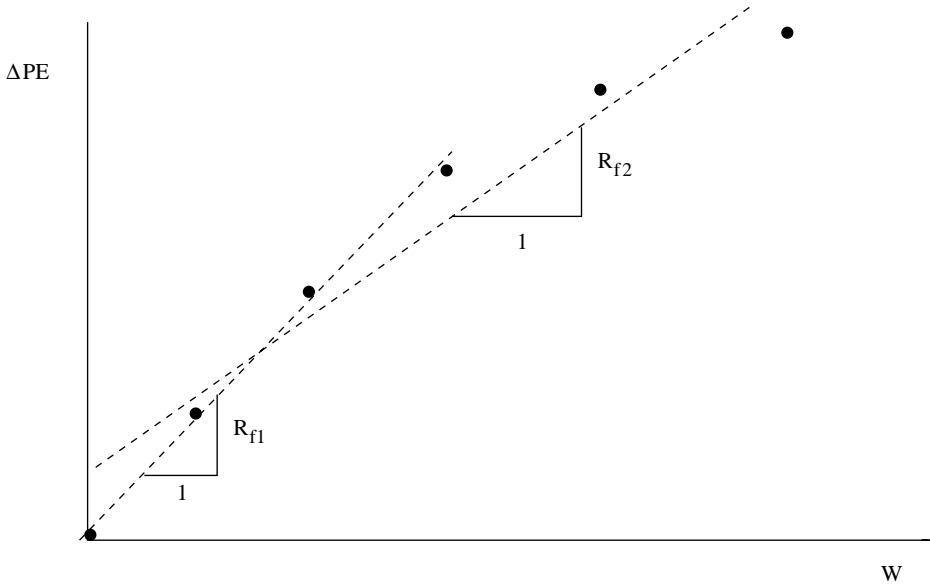


Fig. 2. Comparison of methods to compute the mixing efficiency. When taken as the slope of a line fit to the data, the efficiency depends on the level to which the fluid is mixed, or total amount of work done on the fluid.

estimate the efficiency at zero tows or zero work, as [Rottman and Britter \(1986\)](#) did. In particular, we compute R_f as the slope of the curve at the origin, $W = 0$:

$$R_f = \left. \frac{d(\Delta PE)}{dW} \right|_{W=0}. \tag{6}$$

The eddy diffusivity was computed from the average buoyancy flux during a tow set (e.g., [Barry et al., 2001](#)):

$$K = \frac{\delta PE}{gVT_m(-d\rho/dz)}. \tag{7}$$

The potential energy change δPE was computed with an equation analogous to (5), but with density profiles before and after a tow set. As in [Barry et al. \(2001\)](#), the density gradient was averaged over the fluid volume and over the tow set. The mixing time T_m was estimated as mL_t/U ([Holford and Linden, 1999](#)), where m the number of tows in a set and L_t the length of the tow. [Barry et al. \(2001\)](#) found that the stirring time was within 5% of the duration of the turbulent signal from a conductivity sensor. To evaluate relationships between K and $\epsilon/\nu N^2$, where ϵ is the rate of dissipation of turbulent kinetic energy, an average dissipation was estimated from an energy budget integrated over the duration of the turbulent event and the volume of the fluid. In our terms, the energy budget for a tow set reads

$$\delta W = \delta PE + \int_0^{T_m} \int_V \rho_0 \epsilon \, dV \, dt, \tag{8}$$

where δW is the work done during the tow set. Then, with the definition of the mixing efficiency in (1), the average dissipation is

$$\epsilon_a = \frac{1}{\rho_0 V T_m} (\delta W - \delta PE). \quad (9)$$

Errors in the efficiency and eddy diffusivity measurements consisted mainly of uncertainty in the potential energy change due to internal wave distortion, molecular diffusion of the profile, and bias due to heat losses and probe drift. Although most of the motions vanished by the time profiles were measured, long internal waves persisted. These oscillations hinder profile measurement because they can distort the profile by ‘squeezing and separating’ the constant-density surfaces (Turner, 1979, p. 316). Unless the waves were allowed to decay for a sufficient time, the interface between the mixed layers and the gradient regions appeared very sharp, and the profile appeared to be shifted relative to the initial profile. The decay time was estimated from the analysis of Thorpe (1968) to be between 20 and 40 min for the smallest buoyancy frequencies used in these experiments. An analysis that involves computing the apparent potential energy change due to the longest wave shows that the maximum uncertainty due to waves is about 6% for these experiments, but since the phase of the waves is unknown, the net effect of waves on R_f is uncertain. Waves also contribute to spurious heat fluxes in the sidewall boundary layer, which Jackson and Rehmann (2003b) analyzed in detail. Spurious heat fluxes were less than 3% of the measured heat fluxes in the present experiments.

Bias in the measurements can be caused by molecular diffusion during an experiment and errors in mass conservation, which are due to heat losses in cases with temperature stratification and conductivity sensor drift in cases with salt stratification. Molecular diffusion of the scalar profile will increase the potential energy change and appear to raise the efficiency; the net effect is estimated at between 5 and 10%. Mass was conserved to within 0.03% in the experiments considered in the following analysis. We account for the bias by shifting the density profiles to conserve mass, as Park et al. (1994) did, and treating the difference between potential energy changes computed from shifted and unshifted profiles as a one-sided error. In these experiments, forcing mass conservation causes the potential energy change to increase; that is, the heat losses and probe drift tend to lower the potential energy change artificially. Along with the bias error, we add the uncertainty due to internal wave distortion and molecular diffusion of the profile. Uncertainty in the density and work measurements, including uncertainty due to the extrapolation of the density profiles, was less than about 1%. Accounting for all sources of uncertainty gives a total uncertainty of 10–55% of the mixing efficiency and eddy diffusivity estimates.

3. Results

In this section we discuss the evolution of the density profiles for weakly and strongly stratified flows, and we present measurements of the mixing efficiency and eddy diffusivity to quantify the bulk mixing due to stratified grid turbulence. Results from an experiment with active gradients of both heat and salt are discussed separately.

3.1. Profile evolution

In the cases with moderate stratification density profiles evolved as in the experiments of Britter (1985), Rottman and Britter (1986) and Barrett and Van Atta (1991). Fig. 3a shows profiles from an experiment typical of the cases with $Ri_0 < 1$. In those cases, the turbulence generated a density flux down the gradient. Near the top and bottom of the profiles, where the fluxes must vanish (as long as heat losses are small), mixed layers formed. The density in the upper mixed layer increases because the flux into the layer exceeds the flux out of the layer. For similar reasons, the density in the lower mixed layer decreases. During the first few tows, the gradient in the center of the profile changed little, but later in an experiment, after the mixed layers had grown sufficiently, the gradient decreased. As Rottman and Britter (1986) noted, the profile evolution in these cases superficially resembles what the solution of a diffusion equation would predict, using an eddy diffusivity.

The profile evolution in the three most strongly stratified cases was quite different from that in experiments with smaller Ri_0 . Fig. 3b shows the profiles from an experiment with $Ri_0 = 10.7$, which illustrates the typical behavior for experiments with large Ri_0 . A series of layers and interfaces formed after about twenty tows, and later the layers grew and the interfaces sharpened. After about forty tows the profile changed very little. As in the grid towing experiments of Liu (1995), the layer thickness is approximately equal to the grid mesh for all values of Ri_0 above 0.8. This result contrasts with that from experiments with no imposed vertical scale, in which the layer thickness is proportional to U/N (e.g., Park et al., 1994; Holford and Linden, 1999).

3.2. Mixing efficiency

The mixing efficiency measures the fraction of the work done on the fluid that is used to change the potential energy. A parameter related to the work W_0 done by the grid during one tow is the drag coefficient:

$$C_D = \frac{W_0}{(1/2)\rho_0 U^2 B H L_t}. \quad (10)$$

Barrett and Van Atta (1991) assumed $C_D = 1$ for their grid, while Rottman and Britter (1986) measured $C_D = 1.4$ over a wide range of grid Reynolds numbers. The drag and work measurements obtained directly from the force transducer in our experiments allow the drag coefficient to be computed from the total work done during an experiment with (10). The mean of C_D over several decades of Ri_0 is 1.0 (Fig. 4). The measurements indicate an increase in the drag coefficient for the strongest stratification, as seen in other flows (Turner, 1979, p. 63). However, here C_D depends relatively little on the stratification strength for $Ri_0 < 10$, as Rottman and Britter (1986) observed.

Mixing efficiencies measured in the present and previous grid towing experiments are plotted against Reynolds number and Richardson number in Fig. 5a and b, respectively. In both figures, the results from our experiments are differentiated by salt stratification and temperature stratification. One experiment involved stable profiles of both salt and temperature. The experiments of Britter (1985) and Rottman and Britter (1986) used sodium chloride, while Barrett and Van Atta (1991) used Epsom salt ($MgSO_4$) and sucrose. Parameters of

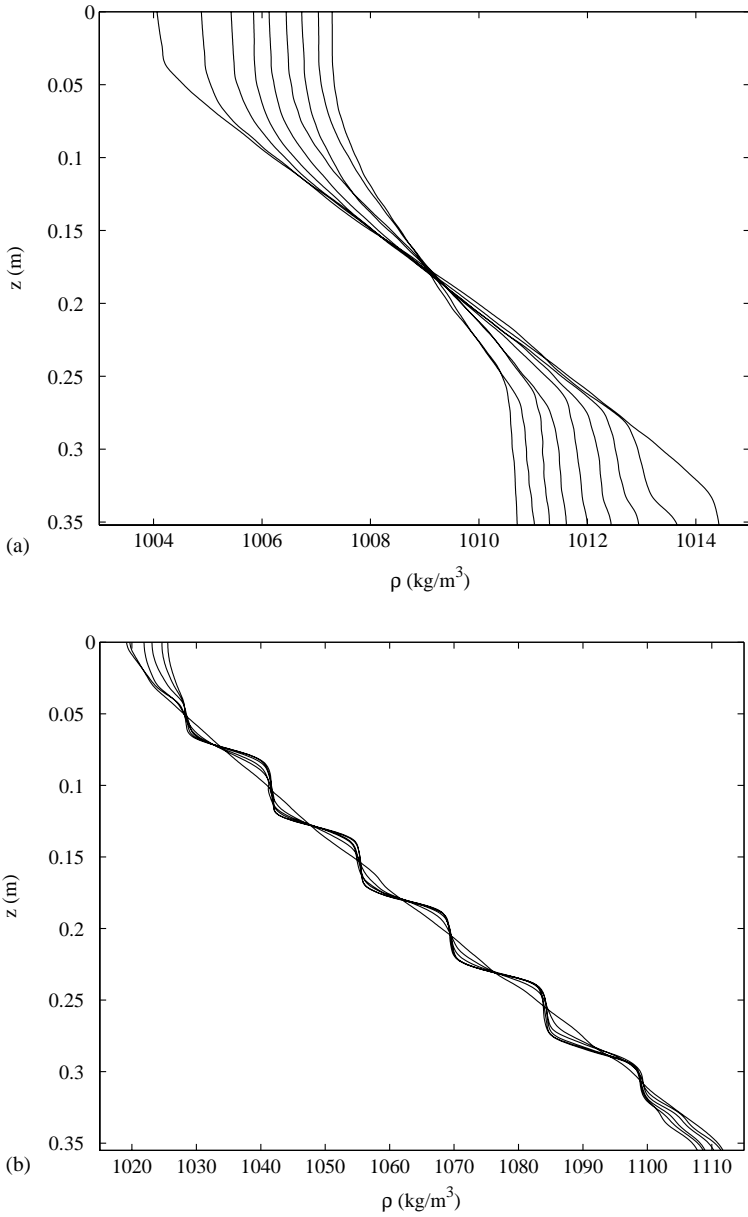


Fig. 3. Examples of the density profile evolution: (a) weak stratification (experiment 1a, $Ri_0 = 0.08$); (b) strong stratification. (experiment 18, $Ri_0 = 10.7$). In both cases, the initial density profile is nearly linear. As the number of tows increases, the density increases near the surface ($z = 0$) and decreases near the bottom.

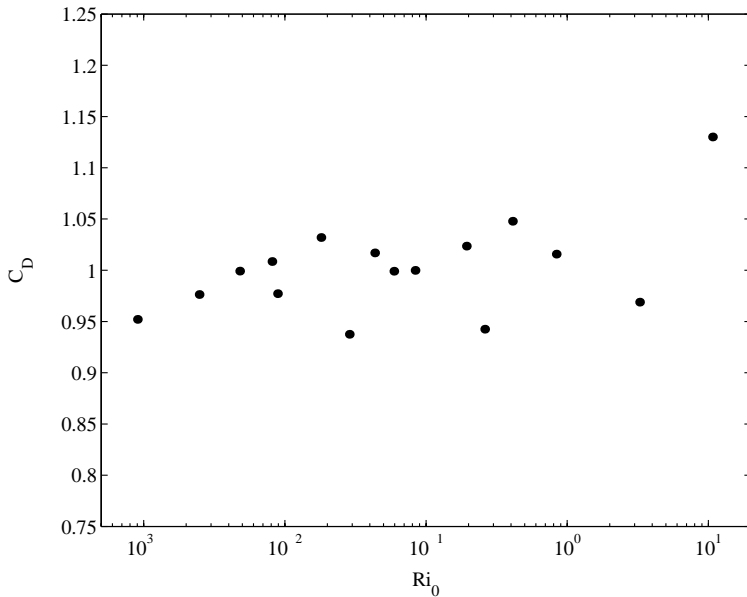


Fig. 4. Drag coefficient as a function of grid Richardson number.

the experiments are summarized in Table 2. The results of Barrett and Van Atta (1991) were adjusted because they measured only the center 25 cm of their 32 cm deep water column. Since most of the change in the density profiles occurs near the boundaries, their measurements underestimate the potential energy change and the mixing efficiency. To compare the results of Barrett and Van Atta (1991) with the other results, an eddy diffusivity that best reproduced the observed profiles over the measured range was determined and used to compute the mixing efficiency as described in Section 2. This analysis showed that their efficiencies will be low by a factor of about 3.3, which was applied to their results in plotting Fig. 5a and b.

Table 2
Parameters used in grid towing experiments

Study	$L \times B \times H$ (m)	U (cm s^{-1})	M (cm)	d (cm)	Re_M	σ (%)
Present study	$4 \times 0.8 \times 0.35$	3–30	5	1	1300–15,400	36
Britter	$25 \times 2.4 \times 1.2$	6–49	8.5	1.9	5100–42,000	40
Rottman and Britter	$25 \times 2.4 \times 1.2$	10–43	8.5	1.9	8600–36,000	40
Barrett and Van Atta	$2.5 \times 0.4 \times 0.32$	43	3.81	0.65	13,000	31

All experiments used square-mesh grids. The bars were square in the present experiments, rectangular in the experiments of Britter (1985), Rottman and Britter (1986), and round in the experiments of Barrett and Van Atta (1991). The bar size d refers to either the bar width or the bar diameter, and the solidity σ the ratio of solid area of the grid to total area. For the experiments of Barrett and Van Atta (1991), the bar diameter was computed from the mesh and solidity they reported.

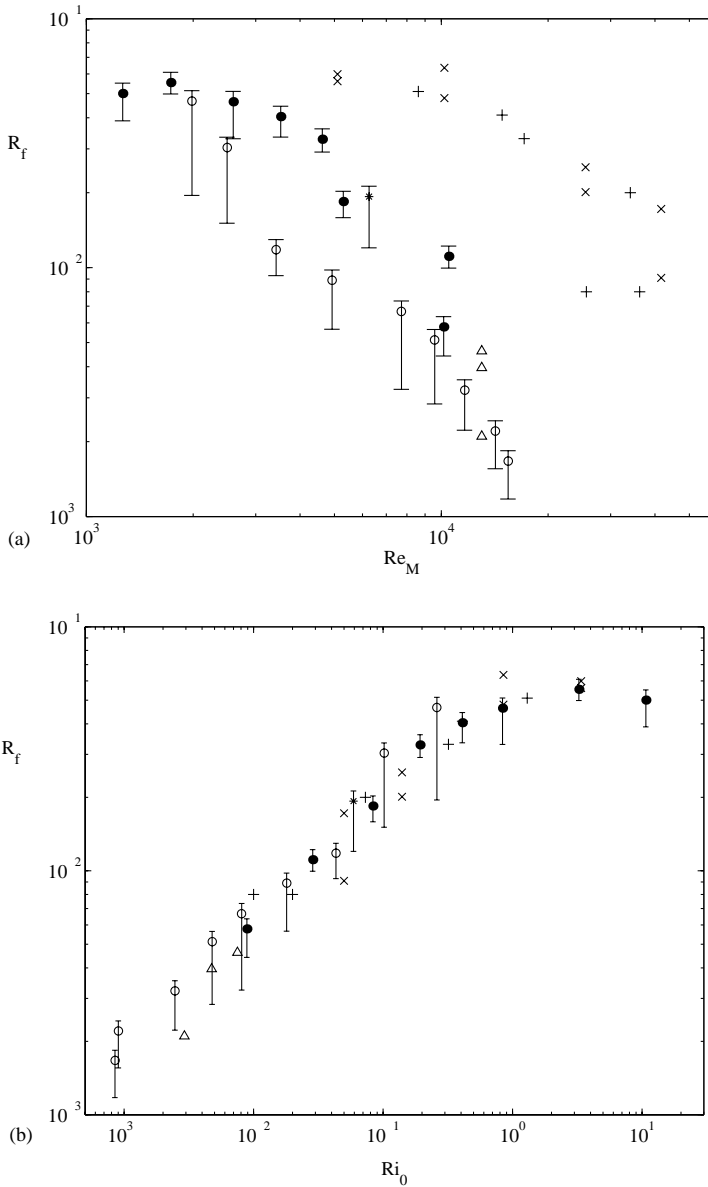


Fig. 5. Mixing efficiency measurements from towed-grid experiments in a linearly-stratified fluid: (a) variation with grid Reynolds number; (b) variation with grid Richardson number. (●) Present data—salt stratification; (○) Present data—temperature stratification; (*) Present data—Salt and temperature stratification (experiment 19); (+) Rottman and Britter (1986); (×) Britter (1985); (△) Barrett and Van Atta (1991). Error bars on the present data and adjustments to the Barrett-Van Atta data are described in the text. A miscalculation of one value of Ri_0 in the data of Rottman and Britter (1986) was corrected (J. Rottman, personal communication, 2003).

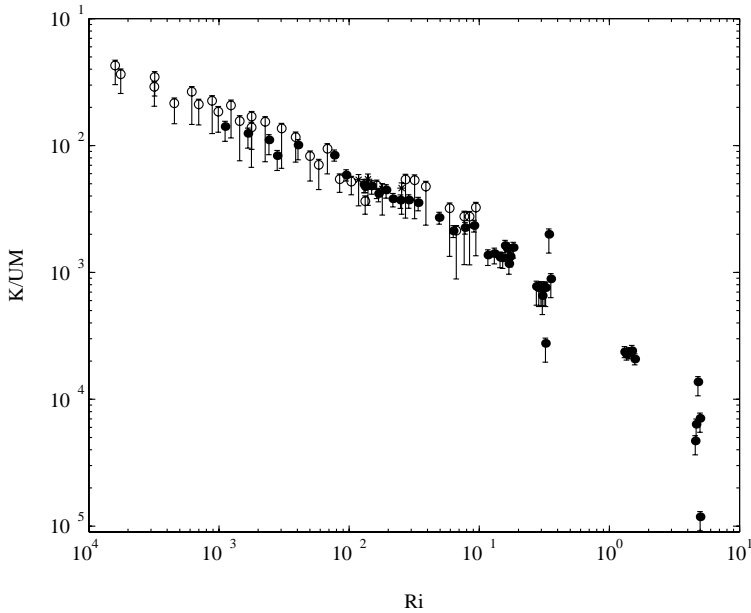


Fig. 6. Dimensionless eddy diffusivity as a function of Richardson number: (●) salt stratification; (○) temperature stratification; (*) salt and temperature stratification (experiment 19).

The efficiency of grid turbulence is quite low. Less than 6% of the work done by the grid is used for mixing over the range of Reynolds and Richardson number shown in Fig. 5. Britter's (1985) arguments suggest that the mixing efficiency will continue to decrease as Ri_0 decreases below 10^{-3} , while Linden's (1979) arguments suggest that the mixing efficiency will eventually decrease as Ri_0 increases beyond our largest value. Therefore, the maximum mixing efficiency for this flow is 6%. This value is much smaller than those for breaking internal waves and shear instabilities (Linden, 1979). Although the grid supplies energy where the mixing occurs, the energy is supplied independently of the flow. For example, much of the energy input by the grid is dissipated close to the grid (e.g., Fig. 6 of Liu, 1995). Although much mixing may occur near the grid, the mixing is not efficient. Also, Stretch et al. (2001) proposed that the generation of internal waves, discussed in Section 2, could remove energy that might otherwise be available for mixing.

The grid Richardson number controls the efficiency of grid turbulence. Although trends between the mixing efficiency and grid Reynolds number can be discerned in Fig. 5a, the efficiencies from the present and previous experiments collapse to a single curve when plotted against Ri_0 (Fig. 5b), as long as the efficiencies are computed in the same way. (The results of Barrett and Van Atta (1991) must also be adjusted, as described above.) Reynolds number effects are minor: At a particular value of Re_M , the efficiency can vary by a factor of 3 in a dataset and by more than an order of magnitude between datasets. At a particular value of Ri_0 , the efficiencies from different runs match well, even though

values of Re_M can differ by up to a factor of 10. Also, the overall mixing does not depend significantly on the solidity of the grid, listed in Table 2. Qualitatively different flow can be generated behind grids of higher solidity (Corrsin, 1963), but for the range used in the towed-grid experiments ($30 < \sigma < 40\%$), the quantitative differences are relatively small.

The variation of the mixing efficiency with the grid Richardson number in our experiments is consistent with that in previous work. For $Ri_0 < 1$ the mixing efficiency increases. Fitting a power law of the form $R_f = aRi_0^b$ to our data for $Ri_0 < 1$ yields exponents of 0.51 ± 0.06 and 0.51 ± 0.05 for the temperature and the salt curves, respectively. (The values of the parameter Q of 0.70 and 0.97 for the respective curves exceed the threshold of 0.1 suggested by Press et al (1986, p. 506) and indicate a good fit.) These exponents are close to the value of 1/2 predicted by Britter (1985) using results from a Lagrangian dispersion analysis and plume dispersion experiments. Testing for a linear relationship between R_f and Ri_0 , which was predicted by Britter (1985), would require experiments with weaker stratifications. However, resolving the potential energy change in experiments with $Ri_0 < 10^{-3}$ is difficult because the entire density profile becomes uniform after a few tows. Practical experimental issues apply to the strongly stratified cases as well. Our experiments show that the efficiency remains constant within experimental uncertainty at slightly higher values of Ri_0 than Britter (1985) and Rottman and Britter (1986) used. Achieving even higher values of Ri_0 is difficult because of the limitations on the maximum salinity difference and minimum grid speed.

Our experiments also suggest that the effects of molecular diffusivity on the overall mixing are relatively small, even though the molecular diffusivity of temperature in water exceeds that of salt in water by a factor of 100. From previous work (e.g., Turner, 1968) effects of molecular diffusivity could be expected to be important when the turbulence is relatively weak, or for high Ri_0 and low Re_M . Indeed, at a particular value of the Reynolds number, the efficiency for a case with temperature stratification is lower or approximately equal to the efficiency for a case with salinity stratification (Fig. 5a). However, these differences are due to differences in Ri_0 : Because large density differences are easier to achieve with salt than with temperature, the velocity or Reynolds number for a temperature-stratified case must be reduced to match values of Ri_0 , and smaller values of Ri_0 lead to smaller efficiencies. Fig. 5b shows that the efficiencies for temperature-stratified and salt-stratified cases agree within the uncertainty of the measurements for $10^{-2} < Ri_0 < 3 \times 10^{-1}$ and grid Reynolds numbers $Re_M = UM/\nu > 2000$.

This finding contrasts with the results of Jackson and Rehmann (2003b), who compared results from runs with several values of a Richardson number and two values of the density ratio $R_\rho = \alpha \Delta T / \beta \Delta S$, where α and β are the coefficients of thermal expansion and haline contraction and ΔT and ΔS are the magnitudes of the total temperature and salinity difference. When both temperature and salinity are stably stratified and α and β are taken as positive, R_ρ defined in this way is positive. Jackson and Rehmann (2003b) found that for low Richardson number, efficiencies from the low R_ρ runs matched those for high R_ρ runs. However, for higher Richardson number, efficiencies for high R_ρ runs were larger. When preferential transport of heat occurs, the potential energy change will be larger when more of the density gradient is due to temperature, or when R_ρ is larger (Jackson and Rehmann, 2003a).

3.3. Eddy diffusivity

Eddy diffusivities in experiments with salinity stratification varied between 1.5×10^{-8} and $1.4 \times 10^{-4} \text{ m}^2 \text{ s}^{-1}$, while eddy diffusivities in cases with temperature stratification varied between 4×10^{-6} and $6 \times 10^{-4} \text{ m}^2 \text{ s}^{-1}$. The minimum eddy diffusivities were 10–25 times the molecular diffusivities of the stratifying agents. For context, Munk (1966) inferred a vertical eddy diffusivity of $O(10^{-4}) \text{ m}^2 \text{ s}^{-1}$ to explain historical temperature profiles in the deep ocean, while eddy diffusivities of $O(10^{-5}) \text{ m}^2 \text{ s}^{-1}$ are measured in the ocean thermocline (Ledwell et al., 1993) and many other parts of the ocean (Gregg, 1998).

Normalized eddy diffusivities are plotted against Richardson number in Fig. 6 and $\epsilon_a/\nu N^2$ in Fig. 7. The Richardson number Ri is computed with the average density gradient during a tow set. The data collapse well except for strong stratification ($Ri > 0.2$). In experiments 2, 17, and 18, which had the strongest stratification, layering occurred and rendered the concept of a bulk eddy diffusivity questionable. The magnitude of K/UM is comparable to that observed in the experiments of Nagata and Komori (2001). Eddy diffusivities computed from their vertical flux measurements yield $0 < K/UM < 5 \times 10^{-3}$ over the approximate Richardson number range $6 \times 10^{-3} < Ri < 8 \times 10^{-2}$. Over the same range bulk diffusivity measurements in our experiments give $2 \times 10^{-3} < K/UM < 7 \times 10^{-3}$.

The eddy diffusivity decreases as the stratification becomes stronger—that is, as Ri increases or $\epsilon_a/\nu N^2$ decreases. For $Ri < 0.2$, $K/UM \propto Ri^{-0.49 \pm 0.02}$. This result can be

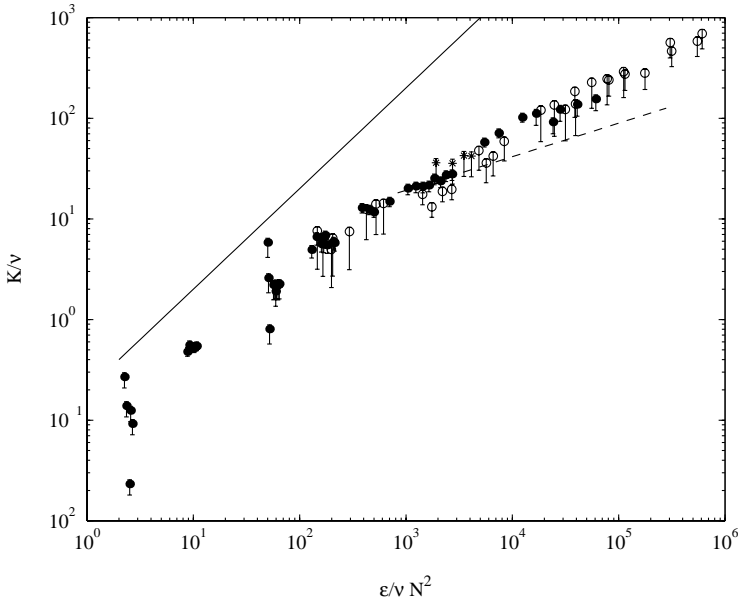


Fig. 7. Dimensionless eddy diffusivity as a function of $\epsilon_a/\nu N^2$: (●) salt stratification; (○) temperature stratification; (*) salt and temperature stratification (experiment 19). The solid line is computed with Osborn's (1980) relation (12) with $\Gamma = 0.2$, and the dashed line is computed with the relation from Barry et al. (2001) for salinity stratification.

related to the mixing efficiency because (7) and (10) can be combined to yield

$$\frac{K}{UM} = \frac{C_D}{2} \frac{M}{L} \frac{\delta PE}{\delta W} Ri^{-1}. \quad (11)$$

As for the mixing efficiency R_f , the exponent in the power law between $\delta PE/\delta W$ and Ri is approximately 1/2. Thus, (11) predicts that K/UM should be proportional to $Ri^{-1/2}$, which agrees well with the measurements. For $\epsilon_a/\nu N^2 > 800$, K/ν increases as $(\epsilon_a/\nu N^2)^{0.60 \pm 0.02}$. This dependence is discussed in the context of oceanographic microstructure methods in Section 4.1

3.4. Mixing of a two-component stratification

The mixing efficiency and eddy diffusivity results in Figs. 5–7 suggest that the effect of the molecular diffusivity on the overall mixing is relatively small, even though one might expect turbulence in a temperature-stratified fluid to be more efficient for the same stirring strength. However, differences between the Richardson and Reynolds numbers between experiments (Table 1) could complicate the interpretation of the results. At the same Ri_0 , a case with temperature stratification tends to have a lower value of Re_M than a case with salinity stratification. Thus, separating the effects of the Reynolds number and Schmidt number is not straightforward.

Experiment 19 was an attempt to eliminate some of the complicating effects. The initial density profile was composed of dynamically active, stable gradients of both temperature and salinity. An advantage of this experiment is that both components experience the same stratification and stirring strength, or Richardson and Reynolds numbers. Another parameter that enters is the ratio of the contributions of the components to the density gradient, or the density ratio R_ρ . In experiment 19, R_ρ was 0.7 initially.

The mixing efficiency and eddy diffusivity for experiment 19 do not differ significantly from the results of the other experiments, as shown in Figs. 5 and 6. However, Fig. 8 shows some effects of differential mixing of temperature and salinity. The T – S diagram, like that in Fig. 8, is used extensively in oceanography to understand the evolution of water masses. In these experiments, if temperature and salinity mixed at the same rate, all profiles would fall on the initial profile, the dashed line in Fig. 8. Mixing would reduce the range of temperatures and salinities and shorten the curve on the T – S diagram. When the profiles became uniform, the curves would shrink to a point. The profiles in Fig. 8 do not collapse on the initial curve. Instead they rotate counterclockwise around the mean temperature and salinity, 28.6 °C and 0.6%. Greater mixing of temperature causes this rotation; for example, the bottom water warms faster than it becomes fresher. Gargett (2003), Jackson and Rehmann (2003b) and Jackson and Rehmann (2003b) give other examples of T – S diagrams that suggest differential diffusion.

To quantify the differences in the mixing of temperature and salinity, eddy diffusivities K_T and K_S for the two components can be computed from expressions analogous to (7) using the first moments of the T and S profiles, and uncertainty can be evaluated as described in Section 2. Values of the diffusivity ratio $d = K_S/K_T$ range from 0.67 to 0.87, though the error bars are large (Fig. 9). Thus, although our results are suggestive of differential diffusion, the effects of heat losses cannot be ruled out conclusively.

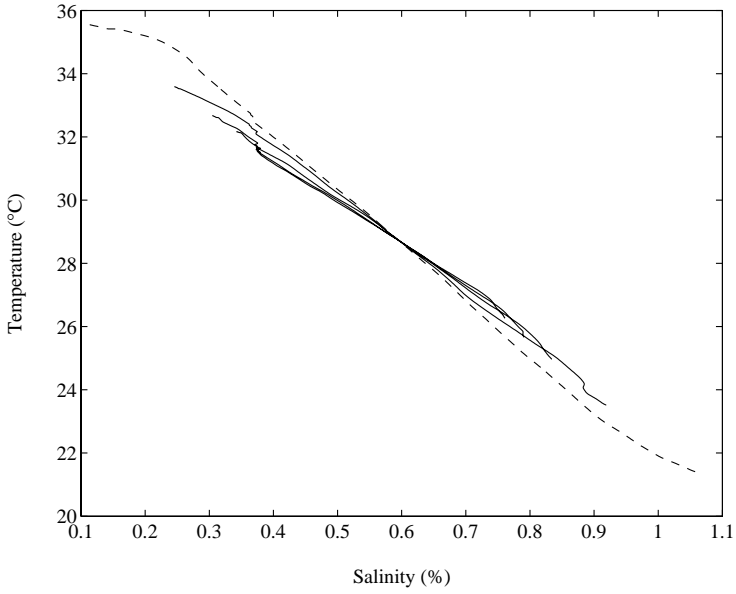


Fig. 8. T – S diagram for experiment 19, which had diffusively-stable, dynamically active temperature and salinity stratification. The initial profile is shown with a dashed line.

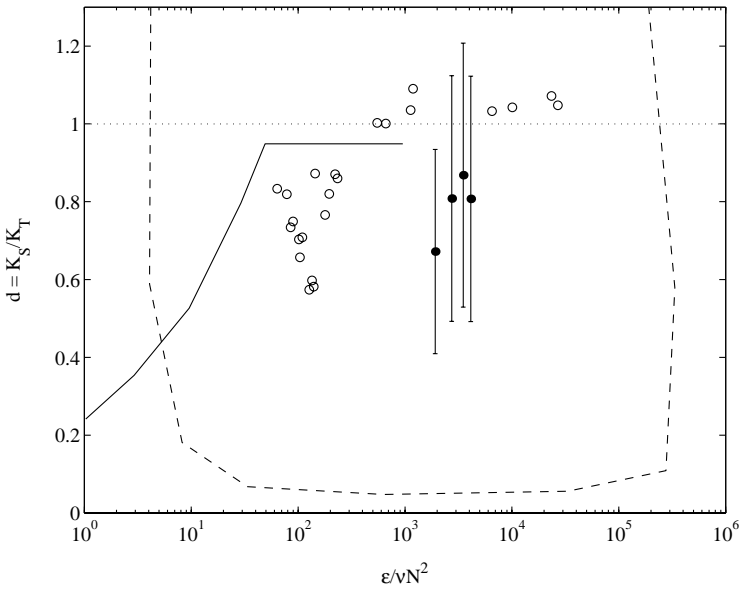


Fig. 9. Comparison of diffusivity ratios from several sources: (●) experiment 19; (○) Jackson and Rehmann (2003b). The solid line represents diffusivity ratios that Nash and Moum (2002) computed from Turner’s (1968) experiments, and the dashed line outlines the range of values from the field measurements of Nash and Moum (2002).

4. Application to oceanography

In this section we discuss our laboratory results in terms of oceanographic applications, including microstructure methods for estimating eddy diffusivity, relationships between K and either the buoyancy frequency or a Richardson number, and differential diffusion.

4.1. Microstructure methods

Oceanographers study vertical mixing by measuring the microstructure of either the velocity or temperature and inferring the eddy diffusivity from the equations of turbulent kinetic energy or temperature variance. For example, [Osborn \(1980\)](#) showed that for stationary, homogeneous flow the eddy diffusivity K_p can be computed with

$$K_p = \Gamma \frac{\epsilon}{N^2}, \quad (12)$$

where $\Gamma = R_f / (1 - R_f)$. This method requires measurements of the dissipation ϵ and an estimate of Γ . [Osborn \(1980\)](#) reviewed theoretical and experimental work on mixing efficiency in shear-driven flows and recommended $\Gamma < 0.2$, or $R_f < 0.15$. Many researchers use this maximum value, while others have used $\Gamma = 0.12$, or $R_f = 0.11$ (e.g. [Wüest et al., 1996](#)).

The values of the mixing efficiency from our experiments are much smaller than those typically used in microstructure measurements. The maximum mixing efficiency of 6% ([Fig. 5](#)) yields $\Gamma < 0.06$. As discussed above, efficiencies tend to be higher for breaking internal waves or flows driven by shear instabilities, which are often cited as causes of vertical mixing in the ocean. However, field measurements and estimates of Γ show a range with low values like those observed in our experiments. The quantity Γ has been computed from directly measured fluxes or by equating eddy diffusivities measured with the [Osborn \(1980\)](#), [Osborn and Cox \(1972\)](#) methods. The values compiled by [Ruddick et al. \(1997\)](#) from several studies range from 0 to 0.35 ($0 < R_f < 0.26$).

In studying methods of estimating vertical diffusivity, [Barry et al. \(2001\)](#) developed a relationship between the eddy diffusivity and parameters of the forcing and stratification. They showed that the [Osborn \(1980\)](#) relation (12) overestimates the eddy diffusivity of grid turbulence if Γ is assumed to be 0.2. They also developed an expression for K_p by assuming inertial scaling for the dissipation, which leads to $K \sim \epsilon^{1/3} L^{4/3}$, and estimating the overturning scale with the convective length scale $L \sim (\nu D)^{1/4} / N^{1/2}$. These estimates yield

$$\frac{K}{\nu^{2/3} D^{1/3}} = 17 \left(\frac{\epsilon_a}{\nu N^2} \right)^{1/3} \quad (13)$$

[Barry et al. \(2001\)](#) showed that (13) collapsed their data for $\epsilon/\nu N^2$ greater than about 800. (Because an error in their energy budget led to an underestimate of the dissipation (G. Ivey, personal communication), the coefficient and region of validity of (13) had to be adjusted.)

The discussion of our mixing efficiency measurements supports the finding that (12) with $\Gamma = 0.2$ overpredicts the eddy diffusivity in grid turbulence ([Fig. 7](#)). However, eddy diffusivities from our experiments do not follow the trend predicted by (13) since the power

law exponent for $\epsilon_a/\nu N^2 > 800$ is 0.60. The assumptions used in developing (13) cannot be tested in our experiments because we did not measure length scales. The dependence found in our experiments is closer to that observed in the numerical simulations of sheared, stratified turbulence (Shih et al., 2003). The numerical results show a regime at low $\epsilon/\nu N^2$ in which the eddy diffusivity is approximately equal to the molecular value, an intermediate regime in which the Osborn (1980) relation holds with lower efficiency, and an energetic regime ($\epsilon/\nu N^2 > 100$) in which the diffusivity is proportional to $(\epsilon/\nu N^2)^{1/2}$.

Although effects of molecular diffusivity are not explicitly included in the Osborn (1980) method, the laboratory experiments allow them to be evaluated. For our experiments eddy diffusivities from cases with temperature stratification match those in cases with salinity stratification within the uncertainty of the experiments (Figs. 6 and 7). In contrast, Barry et al. (2001) found that eddy diffusivities in experiments with water and water-glycerol mixtures stratified with salt collapse when plotted with the scaling in (13); that is, the molecular diffusivity must be included to collapse the results. Our results also differ from those of Nagata and Komori (2001), who found that the eddy diffusivity of heat was smaller than that for passive Fluorescein dye, which has $Sc = O(10^3)$. Differences were relatively small early in the evolution of the turbulence, but numerical simulations showed that they increased with time. Nagata and Komori (2001) attributed the lower diffusivity of the active component (heat) to the restoring effect of buoyancy, which tends to reduce vertical stirring of fluid parcels. In our experiments, temperature and salinity were active scalars, and the eddy diffusivities of salt and temperature agreed at the same stratification strength, measured by either the Richardson number or $\epsilon_a/\nu N^2$.

4.2. Eddy diffusivity

Since ocean circulation models usually cannot resolve the small scales associated with vertical mixing, they often parameterize the mixing with an eddy diffusivity. Reviewing parameterizations of mixing in the ocean interior, Large et al. (1994) considered mixing due to shear-driven turbulence, breaking internal waves, and double diffusion. For shear-driven turbulence, they presented the eddy diffusivity K_{sh} as a function of the gradient Richardson number J , the square of the ratio of the buoyancy frequency and shear rate:

$$\frac{K_{sh}}{K_0} = \left[1 - \left(\frac{J}{J_0} \right)^2 \right]^3, \quad (14)$$

where $K_0 = 5 \times 10^{-3} \text{ m}^2/\text{s}$ and $J_0 = 0.7$. Over the range $0 < J < J_0$, the eddy diffusivity decreases monotonically from a maximum at $J = 0$ to zero at $J = J_0$. Although the processes behind the mixing are different, the eddy diffusivity in grid turbulence also decreases as a Richardson number increases (Fig. 6). The maximum value K_0 , however, is about 10 times greater than the largest diffusivity in our experiments.

Mixing due to breaking internal waves has been parameterized in several ways. Large et al. (1994) simply set the scalar eddy diffusivity to a constant value of $1 \times 10^{-5} \text{ m}^2/\text{s}$. Other relations account for the effect of stratification. For example, internal wave breaking models (e.g., Gargett, 1990; Polzin et al., 1995) can be used with Osborn's (1980) relation (12) to show that $K \propto N^{-a}$ with $0 < a < 1/2$. Measurements of eddy diffusivity above the

bottom boundary layer on the New England Shelf give $K \propto N^{-2.5}$ (Duda and Rehmann, 2002). The eddy diffusivity for grid turbulence decreases more quickly than for breaking internal waves and less quickly than for the coastal ocean measurements. For fixed forcing, the result $K/UM \propto Ri_0^{-0.49}$ (Fig. 6) means the eddy diffusivity is proportional to $N^{-0.98}$ for $Ri_0 < 0.2$.

4.3. Differential diffusion

Recent studies have aimed to identify the conditions under which heat transport exceeds salinity transport. Nash and Moum (2002) measured temperature and salinity microstructure on the Oregon continental shelf and found values of $d < 1$ over four decades in $\epsilon/\nu N^2$; the mean value of d was 0.7, but measurement uncertainty prevented Nash and Moum (2002) from discounting $d \approx 1$. They also used results from the two-layer entrainment experiments of Turner (1968) to show that preferential transport of heat occurs for $\epsilon/\nu N^2 < 100$. This value is uncertain by a factor of about 3 because of the assumptions used in converting Turner's Richardson number to $\epsilon/\nu N^2$. Our direct measurement of the drag force on the grid and the integrated energy budget allow the average dissipation to be estimated more accurately. Jackson and Rehmann (2003b) also avoided some of the uncertainties in our experiments by insulating the free surface with Styrofoam beads and accounting for heat losses in calculating eddy diffusivities. The steady stirring in their experiments allowed the latter to be accomplished. Jackson and Rehmann (2003b) found that differential diffusion occurred for $\epsilon_a/\nu N^2 < 300$. Their results suggest that if our experiments with temperature stratification were run at lower $\epsilon_a/\nu N^2$ differences between eddy diffusivities for temperature and salinity would have appeared.

Although laboratory experiments have identified conditions for differential diffusion to occur, reasons for a critical value of a parameter marking the transition to differential diffusion remain unclear. In analyzing the effect of $\epsilon/\nu N^2$ on the mixing, Nash and Moum (2002) compared the time scale τ_p of a decaying patch to the time τ_θ to cascade scalar variance from the Kolmogorov scale to the Batchelor scale:

$$\frac{\tau_p}{\tau_\theta} \propto \frac{1}{\ln Sc} \left(\frac{\epsilon}{\nu N^2} \right)^{1/2}. \quad (15)$$

This ratio shows that for low $\epsilon/\nu N^2$ and high Sc the patch will decay before the scalar variance is diffused, and differential diffusion is likely to occur. However, specific values of $\epsilon/\nu N^2$ below which differential diffusion occurs cannot be predicted from (15). Rehmann (1995) compared time scales in a similar way but included stirring from the large eddies to the Kolmogorov scale and diffusion across the Batchelor scale. We will present the results of this analysis in a future paper.

Another parameter used to explain effects of molecular diffusivity is the Péclet number $Pe = u\ell/D$, where u and ℓ are velocity and length scales of the turbulence. Crapper and Linden (1974) found that the Péclet number explains the transition between equal and different entrainment rates of heat and salt observed in the oscillating grid experiments of Turner (1968). Also, the thickness h of the density interface, normalized by ℓ , did not depend on the Richardson number, but it did depend on Pe . For $Pe < 200$ (temperature stratification), h/ℓ decreased as Pe increased, but for large Pe (salinity stratification), h/ℓ

was constant. In the low- Pe cases a diffusive core formed at the center of the interface, and the flux was approximately equal to molecular-diffusive flux computed from the observed gradient.

Péclet number effects in our experiments are unclear. The grid Péclet number $Pe_M = UM/D$ was between 1×10^4 and 1×10^5 for cases with temperature stratification and 9×10^5 and 7×10^6 for cases with salinity stratification. In experiment 19, Pe_M for temperature was 4.4×10^4 , and Pe_M for salinity was 100 times larger. Estimating $u \approx 0.08U$ and $\ell \approx 0.5M$ from the experiments of Yoon and Warhaft (1990) at $x/M = 10$ yields Pe for temperature of about 1800. This value exceeds the critical value of 200 found by Crapper and Linden (1974) and suggests that no differential diffusion should occur in experiment 19. However, these arguments are complicated by the decay of the turbulence; though Pe is large initially, it would decrease in the later stages of decay.

The steady stirring in the experiments of Jackson and Rehmann (2003b) removes the complications due to the decaying turbulence. In their most energetic case in which differential diffusion occurred (their experiment 12), Pe for temperature was about 3500, which again exceeds the value found by Crapper and Linden (1974). The value of Pe marking the transition to differential diffusion should not necessarily be the same in the two experiments because of differences between stirring mechanisms and the initial linear and two-layer density profiles. Also, the numerical values of Pe are uncertain in both experiments; Crapper and Linden (1974) obtained u and ℓ from the measurements in an unstratified fluid, and Jackson and Rehmann (2003b) estimated both scales. In any case, unlike the low- Pe runs of Crapper and Linden (1974), none of the cases studied by Jackson and Rehmann (2003b) had significant fluxes due to molecular diffusion; the measured flux was always at least 10 times greater than the molecular-diffusive flux.

5. Summary

We performed laboratory experiments to study the effect of stratification and molecular diffusivity on the mean potential energy change due to grid turbulence. Linear profiles of salt, temperature, or both were established and stirred by towing a vertical, biplane grid horizontally through the fluid. The mixing efficiency R_f was taken as the ratio of the mean potential energy change and the work done by the grid on the fluid. The former quantity was computed from density profiles measured after a set of tows, and the latter was computed directly by integrating force transducer measurements over the length of the tow. Eddy diffusivities were calculated from the average buoyancy flux during a tow set.

The experiments can be separated into weakly and strongly stratified cases. For weakly stratified flows ($Ri_0 < 1$), the density profiles superficially resemble profiles from the solution of a diffusion equation. For strongly stratified flows ($Ri_0 > 1$) sharp interfaces separate weakly stratified layers with a thickness equal to the grid mesh spacing, as Liu (1995) observed. Theories of the layering (e.g., Phillips, 1972; Balmforth et al., 1998) could not be evaluated because the layers were caused by localized mixing behind the horizontal grid bars. For the weaker stratifications, the prediction that $R_f \propto Ri_0^{1/2}$ (Britter, 1985) fits the data rather well, and for strong stratifications ($1 < Ri_0 < 10$) the efficiency is constant within the experimental uncertainty. The efficiency is low ($R_f < 6\%$), and results from

different experiments collapse onto a single R_f – Ri_0 curve if the methods of computing the efficiency are consistent. Within the error and uncertainty of the experiments the efficiencies in temperature-stratified water and salt-stratified water match for $10^{-2} < Ri_0 < 3 \times 10^{-1}$ and grid Reynolds numbers $Re_M = UM/\nu > 2000$.

Eddy diffusivities in experiments with salinity stratification varied between 1.5×10^{-8} and 1.4×10^{-4} m²/s, while eddy diffusivities in cases with temperature stratification varied between 4×10^{-6} and 6×10^{-4} m²/s. Normalized eddy diffusivities decrease with increasing stratification strength—that is, increasing Richardson number or decreasing $\epsilon_a/\nu N^2$. However, the dependence of the eddy diffusivity on both $\epsilon_a/\nu N^2$ and the molecular diffusivity differs from that predicted and observed by Barry et al. (2001). In particular, the eddy diffusivities for temperature and salinity are equal at the same Richardson number or $\epsilon_a/\nu N^2$.

One experiment with dynamically active, stable gradients of both temperature and salinity was performed. Such an experiment allows both components to experience the same stratification and stirring strength, or Richardson and Reynolds numbers. The mixing efficiency and eddy diffusivity from this experiment do not differ significantly from the results of the experiments with single-component stratification. However, the T – S diagram shows that temperature mixes faster than salinity in the case with two-component stratification. The diffusivity ratio K_S/K_T is less than one, but experiments with reduced heat losses are required to conclude definitely that differences between K_T and K_S are significant.

Acknowledgements

We thank Bob Brown for help with building the experimental apparatus, Ryan Jackson for helpful discussions, and the Basic Energy Sciences Program of the US Department of Energy for financial support (grant number DE-FG03-87ER13757). C.R.R. acknowledges support from an Office of Naval Research graduate fellowship.

References

- Balmforth, N.J., Llewellyn Smith, S.G., Young, W.R., 1998. Dynamics of interfaces and layers in a stratified turbulent fluid. *J. Fluid Mech.* 355, 329–358.
- Barrett, T.K., Van Atta, C.W., 1991. Experiments on the inhibition of mixing in stably stratified decaying turbulence using laser Doppler anemometry and laser-induced fluorescence. *Phys. Fluids A* 3, 1321–1332.
- Barry, M.E., Ivey, G.N., Winters, K.B., Imberger, J., 2001. Measurements of diapycnal diffusivities in stratified fluids. *J. Fluid Mech.* 442, 267–291.
- Britter, R.E., 1985. Diffusion and decay in stably-stratified turbulent flows. In: Hunt, J.C.R. (Ed.), *Turbulence and Diffusion in Stable Environments*. Clarendon, Oxford, pp. 3–13.
- Britter, R.E., Hunt, J.C.R., Marsh, G.L., Snyder, W.H., 1983. The effects of stable stratification on turbulent diffusion and the decay of grid turbulence. *J. Fluid Mech.* 127, 27–44.
- Corsin, S., 1963. Turbulence: experimental methods. In: Flügge, S., Truesdell, C. (Eds.), *Handbuch der Physik VIII/2*. Springer, Berlin, pp. 524–590.
- Crapper, P.F., Linden, P.F., 1974. The structure of turbulent density interfaces. *J. Fluid Mech.* 65, 45–63.
- Duda, T.F., Rehmann, C.R., 2002. Systematic microstructure variability in double-diffusively stable coastal waters of nonuniform density gradient. *J. Geophys. Res.* 107, 3145. Doi:10.1029/2001JC000844.
- Fernando, H.J.S., 1991. Turbulent mixing in stratified fluids. *Annu. Rev. Fluid Mech.* 23, 455–493.

- Gargett, A.E., 1990. Do we really know how to scale the turbulent kinetic energy dissipation rate ϵ due to breaking of oceanic internal waves? *J. Geophys. Res.* 95, 15,971–15,974.
- Gargett, A.E., 2003. Differential diffusion: an oceanographic primer. *Prog. Oceanogr.* 56, 559–570.
- Gregg, M.C., 1987. Diapycnal mixing in the thermocline: a review. *J. Geophys. Res.* 92, 5249–5286.
- Gregg, M.C., 1998. Estimation and geography of diapycnal mixing in the stratified ocean. In: Imberger, J. (Ed.), *Physical Processes in Lakes and Oceans*. American Geophysical Union, Washington, DC, pp. 305–338.
- Hebert, D., Ruddick, B.R., 2003. Differential mixing by breaking internal waves. *Geophys. Res. Lett.* 30, Doi:10.1029/2002GL016250.
- Holford, J.M., Linden, P.F., 1999. Turbulent mixing in a stratified fluid. *Dyn. Atmos. Oceans* 30, 173–198.
- Huq, P., Britter, R.E., 1995. Turbulence evolution and mixing in a two-layer stably stratified fluid. *J. Fluid Mech.* 285, 41–67.
- Jackson, P.R., Rehmann, C.R., 2003a. Kinematic effects of differential transport on mixing efficiency in a diffusively stable, turbulent flow. *J. Phys. Oceanogr.* 33, 299–304.
- Jackson, P.R., Rehmann, C.R., 2003b. Laboratory measurements of differential diffusion in a diffusively-stable, turbulent flow. *J. Phys. Oceanogr.* 33, 1592–1603.
- Large, W.G., McWilliams, J.C., Doney, S.C., 1994. Oceanic vertical mixing: a review and a model with a nonlocal boundary layer parameterization. *Rev. Geophys.* 32, 363–403.
- Ledwell, J.R., Watson, A.J., Law, C.S., 1993. Evidence for slow mixing across the pycnocline from an open-ocean tracer-release experiment. *Nature* 364, 701–703.
- Lienhard V, J.H., Van Atta, C.W., 1990. The decay of turbulence in thermally stratified flow. *J. Fluid Mech.* 210, 57–112.
- Linden, P.F., 1979. Mixing in stratified fluids. *Geophys. Astrophys. Fluid Dyn.* 13, 3–23.
- Linden, P.F., 1980. Mixing across a density interface produced by grid turbulence. *J. Fluid Mech.* 100, 691–703.
- Liu, H.-T., 1995. Energetics of grid turbulence in a stably stratified fluid. *J. Fluid Mech.* 296, 127–157.
- Merryfield, W.J., Holloway, G., Gargett, A.E., 1998. Differential vertical transport of heat and salt by weak stratified turbulence. *Geophys. Res. Lett.* 25, 2773–2776.
- Munk, W.H., 1966. Abyssal recipes. *Deep Sea Res.* 13, 707–730.
- Nagata, K., Komori, S., 2001. The difference in turbulent diffusion between active and passive scalars in stable thermal stratification. *J. Fluid Mech.* 430, 361–380.
- Nash, J.D., Moum, J.N., 2002. Microstructure estimates of turbulent salinity flux and the dissipation spectrum of salinity. *J. Phys. Oceanogr.* 32, 2312–2333.
- Osborn, T.R., 1980. Estimates of the local rate of vertical diffusion from dissipation measurements. *J. Phys. Oceanogr.* 10, 83–89.
- Osborn, T.R., Cox, C.S., 1972. Oceanic fine structure. *Geophys. Fluid Dyn.* 3, 321–345.
- Park, Y.-G., Whitehead, J.A., Gnanadesikan, A., 1994. Turbulent mixing in stratified fluids: Layer formation and energetics. *J. Fluid Mech.* 279, 279–311.
- Pearson, H.J., Puttock, J.S., Hunt, J.C.R., 1983. A statistical model of fluid-element motions and vertical diffusion in a homogeneous stratified turbulent flow. *J. Fluid Mech.* 129, 219–249.
- Phillips, O.M., 1972. Turbulence in a strongly stratified fluid—is it unstable? *Deep Sea Res.* 19, 79–81.
- Polzin, K.L., Toole, J.M., Schmitt, R.W., 1995. Finescale parameterizations of turbulent dissipation. *J. Phys. Oceanogr.* 25, 306–328.
- Posmentier, E.S., 1977. The generation of salinity finestructure by vertical diffusion. *J. Phys. Oceanogr.* 7, 298–300.
- Press, W.H., Flannery, B.P., Teukolsky, S.A., Vetterling, W.T., 1986. *Numerical Recipes*. Cambridge University Press, Cambridge, UK
- Rehmann, C.R., 1995. Effects of stratification and molecular diffusivity on the mixing efficiency of decaying grid turbulence. Ph.D. Thesis, Stanford University.
- Rottman, J.W., Britter, R.E., 1986. The mixing efficiency and decay of grid-generated turbulence in stably-stratified fluids. In: *Proceedings of the Ninth Australasian Fluid Mechanical Conference*, University of Auckland, Auckland, NZ, pp. 218–221
- Ruddick, B.R., Shirtcliffe, T.G.L., 1979. Data for double diffusers: Physical properties of aqueous salt-sugar solutions. *Deep Sea Res.* 26A, 775–787.
- Ruddick, B., Walsh, D., Oakey, N., 1997. Variations in apparent mixing efficiency in the North Atlantic Central Water. *J. Phys. Oceanogr.* 27, 2589–2605.

- Saylor, J.R., Sreenivasan, K.R., 1997. Differential diffusion in low Reynolds number water jets. *Phys. Fluids* 10, 1135–1146.
- Schmitt, R.W., 1994. Double diffusion in oceanography. *Annu. Rev. Fluid Mech.* 26, 255–285.
- Shih, L.H., Koseff, J.R., Ivey, G.N., Ferziger, J.H., 2003. Parameterization of turbulent fluxes and scales using homogeneous sheared stratified turbulence simulations. *J. Fluid Mech.* Submitted
- Stretch, D.D., Rottman, J.W., Nomura, K.K., Venayagamoorthy, S.K., 2001. Transient mixing events in stably stratified turbulence. In: *Proceedings of the 14th Australasian Fluid Mechanical Conference*, Adelaide University, Adelaide, Australia.
- Thorpe, S.A., 1968. On standing internal gravity waves of finite amplitude. *J. Fluid Mech.* 32, 489–528.
- Turner, J.S., 1968. The influence of molecular diffusivity on turbulent entrainment across a density interface. *J. Fluid Mech.* 33, 639–656.
- Turner, J.S., 1979. *Buoyancy Effects in Fluids*. Cambridge University Press, Cambridge, UK.
- Wüest, A., van Senden, D.C., Imberger, J., Piepke, G., Gloor, M., 1996. Comparison of diapycnal diffusivity measured by tracer and microstructure techniques. *Dyn. Atmos. Oceans* 24, 27–39.
- Yoon, K., Warhaft, Z., 1990. The evolution of grid-generated turbulence under conditions of stable thermal stratification. *J. Fluid Mech.* 215, 601–638.